

# Kinematics and Performance of Maneuvering Control Surfaces in Teleost Fishes

Jeffrey A. Walker

**Abstract**—Many fishes routinely exploit resources in high-energy marine habitats of interest to ocean engineers, including rocky coasts and coral reefs. How fishes modulate fin motions to correct perturbations to the preferred heading or to maneuver in complex structure should interest both biologists and ocean engineers. These fin motions are reviewed in order to generate simple models of causal relationships between fin design, motion, and maneuvering performance. The available data on maneuvering performance in fishes is reviewed to compare to the simple models, to identify gaps in our knowledge, and to outline a research program to address these gaps more effectively.

**Index Terms**—Fish, kinematics, maneuvering, pectoral fins, review.

## I. INTRODUCTION

TELEOST fishes present a wide diversity of both maneuvering behaviors and hydrodynamic mechanisms to control maneuvering. Maneuvering behaviors include small yaw and pitch turns that either correct perturbations to some desired heading or reorient fish in a new heading; large yaw and pitch turns that are used to reverse direction; rapid yaw turns that are used for escape from a threatening stimulus; rapid accelerations for escape or the pursuit of prey; braking, reversing, and hovering in still water; or a bidirectional surge. The ability to exploit resources in structurally complex and high-energy habitats such as wave-swept rocky shores and coral reefs using a diverse repertoire of maneuvering behaviors suggests that fishes are a good model for transferring biological information to the design and control of autonomous underwater vehicles (AUVs). While the entire body and fin surface of fishes function in maneuvering control, the combination of fin and body motions necessary to actuate a maneuver differ both within individuals among behaviors and within behaviors among individuals and species. A qualitative comparison of swimming behavior among a diverse array of fishes suggests two general principles. First, while axial (body) undulations are used by most fishes for steady swimming at typical cruising speeds, maneuvers are commonly controlled by fin motions with or without axial bending. Second, the tremendous variation in the combination of fin shapes and motions suggest that no single phenotype is optimal for the complete suite of maneuvering behaviors. The goal of this paper, then, is not to suggest the best species for an AUV blueprint, because the design of any one species reflects both the distinct

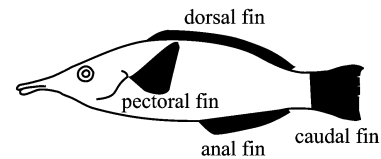


Fig. 1. Principal control surfaces of teleost fishes.

signature of its history and a mind-boggling array of tradeoffs due to competing demands on functional systems. Instead, the goal of this paper is to review the kinematic control mechanisms used for maneuvering, compare the performance consequences of this variation, and use general principles distilled from these studies to suggest biology-inspired technologies for AUV design that best match the desired function. Because current AUV designs are based on rigid bodies, I will emphasize fin-actuated maneuvers in this review, but comparisons will be made with body-actuated maneuvers to assess potential performance tradeoffs due to rigid bodies. The relevant fins are illustrated in Fig. 1. Detailed descriptions of the fluid dynamics of either fin- or axial-powered propulsion and maneuvering are treated in other reviews [1]–[3].

## II. CONTROL SURFACE MOTIONS

### A. Body and Caudal Fin (BCF) Motion

Axial deformations are used for yaw turns in nearly all fishes and braking [4], [5] and reversing [6] in some fishes. Following [7] and [8], I refer to axial bending powered maneuvers as BCF maneuvering. The surfaces of median and caudal fins in BCF maneuvering are generally treated as stiff extensions of the body and without independent actuation mechanisms. Deformations of the caudal fin *sensu stricto* will not be reviewed here, but have been discussed in [9]. Median fin motions by muscles that directly actuate the median fin bony rays are described below.

The BCF control of routine turns has not been systematically investigated, but qualitative and quantitative descriptions of axial bending and turning behavior have been described [10]–[12]. BCF motions that generate large accelerations and rapid rotations have been intensely investigated. A brief description of the kinematics is given here, but the reader is referred to the thorough review in [13]. There are two general kinematic modes of BCF powered accelerations: C starts, which are generally associated with startle or escape responses, and S starts, which are generally associated with predation strikes. A C start is typically divided into three stages [10]. In stage I, the axial muscles along all or most of one side contract strongly, which bends the fish into a C shape. This initial bending might result from either simultaneous muscle contraction along the

Manuscript received October 10, 2003; revised May 19, 2004. This work was supported in part by the U.S. Office of Naval Research under Contract N00014-01-1-0506 and Contract N00014-03-1-0004.

The author is with the Department of Biology, University of Southern Maine, Portland, ME 04103 USA (e-mail: walker@usm.maine.edu).

Digital Object Identifier 10.1109/JOE.2004.833217

axis or a very rapid moving wave. In stage II, a large-amplitude traveling wave of contralateral muscle contraction rapidly passes from anterior to posterior. Stage III is variable, but can include braking, gliding to a stop, small-to-moderate axial undulations that maintain swimming speed, or moderate to large amplitude axial undulations that continue to accelerate the fish. S-start kinematics differ mainly in the S shape that occurs at the end of stage 1.

### B. Median and Paired Fin (MPF) Motions

Fin anatomy is highly relevant to fin motions and is reviewed by Lauder and Drucker [1] and Westneat *et al.* [14]. The fins of actinopterygian (bony ray) fishes are supported and controlled by multiple bony rods or fin rays. Four muscles insert onto the base of each ray, potentially allowing a full two degrees of freedom at each fin ray joint. Qualitative investigations of fin motions suggest that fishes have large control over the patterns of fin muscle activation and, ultimately, fin deformations (hence, reducing the influence of external fluid dynamic and internal elastic stresses). Consequently, fin motions of fishes can be much more complex than the typical heaving and pitching motions of rigid wings or even chordwise flexible wings controlled at a single support axis. Not surprisingly, the kinematics of the fin motions varies tremendously within and among individuals, populations, and species.

1) *Median Fin Deformations*: Median fins vary greatly in both shape and deformations (both rigid body deformations, including oscillation and pitching, and nonuniform deformations of the surface, including undulations). Much of the recent focus on median fins has been on the kinematic, fluid dynamic, and performance differences between long-based, low-aspect ratio (AR), undulatory median fins and long-based, high-AR, flapping median fins [15]–[18]. But median fin shape and motion are highly variable. The “soft” posterior portion of the dorsal fin in the bluegill sunfish oscillates independently of the body and contributes to the thrust balance during steady swimming [19]. The short-based fan-shaped median fins (or pectoral fin) of boxfishes, pufferfishes, and burrfishes contribute to the thrust balance during steady swimming [20]–[22] and are active during yaw-turning maneuvers [23].

More relevant to this review are the dorsal and anal fin motions that contribute to maneuvering. Following a pectoral fin actuated yaw rotation of small magnitude (about  $25^\circ$ ) while swimming in a slow current (0.5 L/s), the soft (posterior) portion of the median fin of the bluegill sunfish rapidly abducts in a direction opposite that of the turn [19]. The median fin motion generates a force directed medially and anteriorly, generating a torque of the opposite sign to that generated by the pectoral fins. This torque would have the effect of returning the heading back to a direction parallel with the flow.

Breder [24] suggested that the median fins of tetraodontids (pufferfishes) could generate yaw-rotational torques by limiting oscillation to the side of the mid-sagittal plane in which the fish is turning. It would seem that limiting the motion to one side of the mid-sagittal plane is not necessary if the fin can create unbalanced forces when oscillating to one side versus the other. Because of their very narrow base and distally expanded paddle-shaped surface, the median fins of pufferfishes,

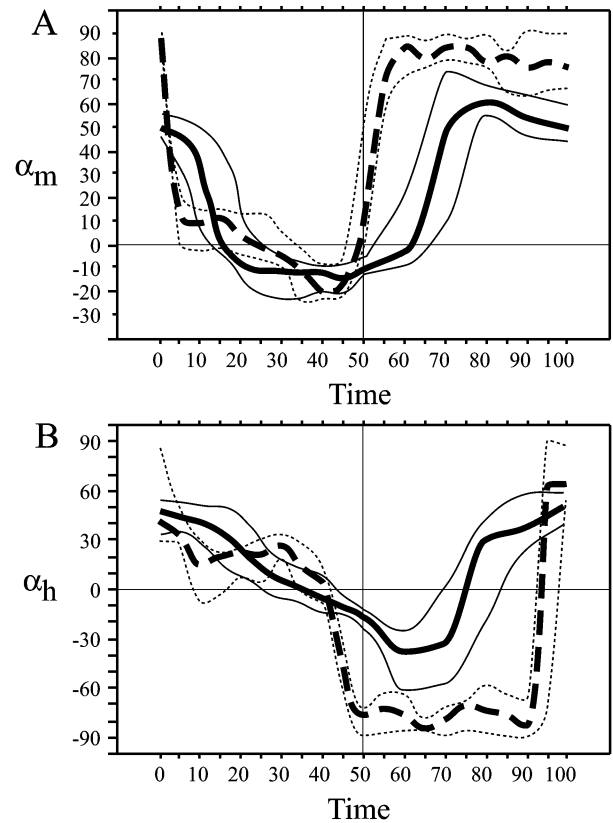


Fig. 2. Morphological (A) and hydrodynamic (B) angles of attack for the rowing stroke of the threespine stickleback (dashed lines), *Gasterosteus aculeatus*, and the flapping stroke of the bird wrasse (solid lines), *Gomphosus varius*. The thick lines represent the mean attack angles while the thin lines represent the 90% confidence intervals. Modified from [28].

boxfishes, and burrfishes should be able to translate broadside during one stroke and feathered during the opposite stroke. The illustration of dorsal and anal fin motion during yaw turning in the boxfish *Tetrasomus gibbosus* suggests that these fins neither feather during one stroke nor limit their motion to one side of the midsagittal plane [23]. The illustration of the *T. gibbosus* dorsal fin does show that the posterior region of the fin base can be actively rotated relative to the anterior region by about  $40^\circ$ .

2) *Pectoral Fin Deformations*: Deformations of the pectoral fins during steady swimming have been described in great detail and are reviewed here in order to facilitate the discussion of the motions during maneuvering.

a) *Pectoral fin deformations during steady swimming*: Most of the focus on variation in pectoral fin motion has been on hydrodynamic, performance, and ecological differences between “rowing” along a horizontal stroke plane and “flapping” along a vertical stroke plane [24]–[31] during steady swimming. Both rowing and flapping include heaving (root oscillation of the fin back and forth along the stroke plane) and pitching (rotation of the fin around a spanwise axis) motions (Fig. 2). The stroke plane is constrained by the geometry of the fin-ray joint within the fibrocartilage pad of the shoulder plate, the orientation of the fibrocartilage pad, and by the mobility of the joints within the shoulder plate (four bony radials and the fibrocartilage pad) [1]. The fin-ray joints allow a large major axis of motion (that occurring along the stroke plane) and a smaller

minor axis of motion (normal to the stroke plane). The fibrocartilage pad is curved [32], which might create variation in the major axis of mobility among the rays. The surface swept out by the leading edge of a pectoral fin is not a plane, but a slightly curved surface that is inclined more vertically during fin abduction and more horizontally during fin adduction [22], [33]–[38]. The difference between the abduction stroke plane angle and adduction stroke plane angle is greater in fishes that present more of a rowing stroke [38]. The orientation of the abduction and adduction stroke planes can also vary among strokes, typically as a function of swimming speed [22], [38]. Fishes at the rowing–flapping extremes, such as the threespine stickleback, a stereotypical rower, and the bird wrasse, a stereotypical flapper, present little variation in stroke plane angle with speed [28]. By contrast, fishes that are more intermediate between rowing and flapping may either decrease [22] or increase [38] the steepness of the stroke plane as speed increases (although the stroke plane angles never reach the extremes of the stickleback and the bird wrasse). The anatomical mechanism allowing this limited variation in stroke plane angle within individuals has not been investigated, but could include both rotation of the fin root (the fibrocartilage pad) and some component of fin–ray motion along the minor axis of the fin ray joint. No substantial ( $>5^\circ$ ) fin-root rotation was noticed in threespine sticklebacks or the wrasses (Walker, unpublished observations), but large root rotations (up to  $30^\circ$ ) have been illustrated for boxfish [23] and trout [39]. It should be noted that the mean stroke plane angle (the mean of the abduction and adduction stroke plane angles) is not perpendicular to the major axis of the fin root, but there is a correlation between the orientation of the fin root and this mean angle among species [31].

Reorientation of the fin root at the shoulder plate is one of two mechanisms for pitching the fin. Rotation of the fin root rotates the fin uniformly along the span and is, therefore, functionally similar to the pitching mechanism found in insect wings and motorized oscillating fins such as those in a robotic fruit fly [40] and bass [41], [42]. The degree to which fish can rotate the fin root has not been investigated and probably varies among species as a function of shoulder-plate mobility [43], [44]. Regardless of the amount of rotation at the fin root, the primary mechanism that fish exploit to pitch the fin is by controlling the phase variation between leading and trailing fin rays (as described for fin undulation previously). The larger the phase lag between the leading and trailing edge (up to  $180^\circ$ ), the larger the pitch amplitude. Unlike rotation of the fin root, however, this mechanism does not rotate the fin as a rigid plate, but dynamically twists the fin along its span. The twisting generates a spanwise gradient of chord pitch amplitudes; the pitch amplitude is necessarily zero at the fin root (i.e., all pitching at the root must come from reorientation of the fin root) and increases to its maximum, which should occur not at the fin tip, but at the spanwise location containing the tip of the trailing edge ray. Because of the separate tendinous insertion of the abductor and adductor muscles on each ray, actinopterygian fishes should have large active control of the deformations that generate this spanwise gradient of pitch.

The pitch, or orientation, of a chordwise segment relative to a horizontal (frontal) plane at time  $t$  and spanwise position  $r$  is

$\alpha_m(t, r)$ . The change in  $\alpha_m$  during a stroke cycle for a distal chord element is not a simple harmonic function for either an extreme rower (three-spine stickleback) or an extreme flapper (bird wrasse; Fig. 2). For a rowing fin, we expect this from the simple principle that mean thrust should be maximized by minimizing  $\alpha_m$  (i.e.,  $\alpha_m = 0^\circ$ ) throughout the recovery stroke and maximizing  $\alpha_m$  (i.e.,  $\alpha_m = 90^\circ$ ) throughout the power stroke. Indeed, we find this general pattern in the stickleback (Fig. 2). In the stickleback,  $\alpha_m$  rapidly falls from  $90^\circ$  to  $10^\circ$  at the beginning of the recovery stroke, gradually drops to  $-20^\circ$  at the end of the recovery stroke, and rapidly climbs to and is maintained at  $85^\circ$  at the beginning of the power stroke. The negative  $\alpha_m$  for the distal element during the recovery stroke reflects a constraint of using a phase lag between leading and trailing edge to generate fin pitch. The fin root of the stickleback is oriented about  $70^\circ$  from the horizontal. Were the fin root able to rotate to  $0^\circ$ , the entire fin could optimally feather (i.e.,  $\alpha_m = 0^\circ$ ) during the recovery stroke. By twisting the fin, optimum feathering during the recovery stroke can only occur at a single spanwise position;  $\alpha_m$  will be greater than zero proximal to this position and less than zero distal to this position. The spanwise position of this optimum, which will ultimately determine the abduction pitch amplitude at the fin tip, is that point that minimizes the integral of  $cU^2|\alpha_m|$  along the span, where  $c$  is the fin chord,  $U$  is the tangential velocity of the fin element and the brackets represent the absolute value.

In the bird wrasse,  $\alpha_m$  rapidly drops to about  $-10^\circ$  during the downstroke and maintains this level until the beginning of the upstroke. About halfway through the upstroke,  $\alpha_m$  reaches its peak of  $60^\circ$ . As predicted by a simple rowing–flapping model [26], [28], the upstroke  $\alpha_m$  is substantially less than the power stroke  $\alpha_m$  of the bird wrasse. Nevertheless, an asymmetry between downstroke and upstroke  $\alpha_m$  differs from the symmetric angles predicted by an idealized neutrally buoyant flapping fin (that is, the absolute value of the positive and negative pitch amplitudes should be the same). Indeed, this difference from the idealized model reflects the negative buoyancy of the bird wrasse and the necessity of generating a net upward force during the stroke cycle. As in birds and insects, the stroke-plane angle of the bird wrasse is tilted back to create an upward component to the mean force over a stroke cycle. The stroke plane angle of the bird wrasse is about  $20^\circ$  from the vertical [37], while the  $\alpha_m$  peaks are symmetric about a midpoint of  $25^\circ$  (Fig. 2).

A spanwise twist mechanism of pitch control should be more effective than a root-rotation mechanism of pitch control for flapping propulsion if there is a strong spanwise gradient in the angle of the incident flow. This might occur, for example, at moderate advance ratios, where the flapping component of the incident flow dominates at the tip while the translational component of the incident flow dominates at the fin base. Given the change in the incident flow angle down the span, the spanwise twist allows the fin pitch to match the optimal pitch, which also changes (increases) down the span. Indeed, spanwise twisting is a common feature of the flapping stroke among many aquatic animals other than fishes, including pteropod gastropods, finned cephalopods, and sea turtles (see references in [27] and [45]). In contrast, at low advance ratios, a root-pitching fin may be more effective because large incident flows at high angles (and,

consequently, forces) would occur along the entire span during the rotational phases of the stroke cycle. This stroke geometry would allow the animal to take advantage of the large rotational forces occurring during rotational phases. Importantly, differences in the timing and duration of the rotational phases between fins have been shown to be important for insect maneuverability [46]. Even fishes without a root-pitching fin could exploit this rotational mechanism if the trailing edge ray is short relative to the leading edge ray (a geometry that would allow the fin distal to the trailing edge tip to rotate semi-rigidly). For example, during steady swimming in the bird wrasse, the distal fin chord does not pitch with a substantially larger amplitude than the proximal fin chord (located at the spanwise position of the tip of the trailing edge ray), indicating that much of the fin is rotating semi-rigidly (see [37, Fig. 13]).

A root-pitch mechanism is more effective for rowing because this allows perfect feathering along the span during the recovery stroke and perfect broadside orientation during the power stroke [27]. In many animals with spanwise segmented limbs that have mobile intersegmental joints, including some mammals [47], freshwater turtles [48], and large water beetles [49], [50], only the distal segment is expanded into a propulsive paddle. “Root” pitching rotation of the stiff (untwisted) distal segment occurs by rotation at one or more intersegmental joints.

Root pitching is only effective when the joint allowing pitching rotation is distal to the joint allowing limb heaving (that is, the pitching joint oscillates with the limb). This geometry occurs in beetles and tetrapods, but not actinopterygian fishes. Root rotation in fishes would require that the fin rays oscillate along the minor axis of the fin ray joint during the recovery stroke and along the major axis of the joint during the power stroke. The elliptical geometry of the fin ray joints do not allow large motions along the minor axis. Hence, for rotation to be effective in fishes, the fin-ray joints would have to have a ball-and-socket geometry, which would most likely compromise the stability of the joint when highly loaded.

While the root-pitching mechanism of pitch control is optimal for the translation phases of the stroke cycle, the spanwise twisting mechanism may actually be more effective during the stroke transition phases. This is because a root-pitching fin, at least one that is rigidly rotating as in the fruit fly, will generate large vertical in addition to horizontal forces, which is good if large lift is desired, but wasted energy if it is not [40], [51], [52] (Fig. 3). For example, at the beginning of the transition to the power stroke, clockwise rotation (in the left lateral view) about the leading edge will generate an upward force and a horizontal force with a large drag and small medial component (Fig. 3). In contrast, rapid clockwise rotation about the trailing edge will generate a downward force and a horizontal force with moderate thrust and small lateral components (Fig. 3). Similarly, at the beginning of the transition to the recovery stroke, when the fin initiates movement away from the body, counterclockwise rotation of the fin about the trailing edge will generate an upward force in addition to a horizontal force with a large medial and small drag component. Rapid counterclockwise rotation about the leading edge would generate a downward force in addition to a horizontal force with a large lateral and small thrust component (this is not illustrated, but is simply opposite

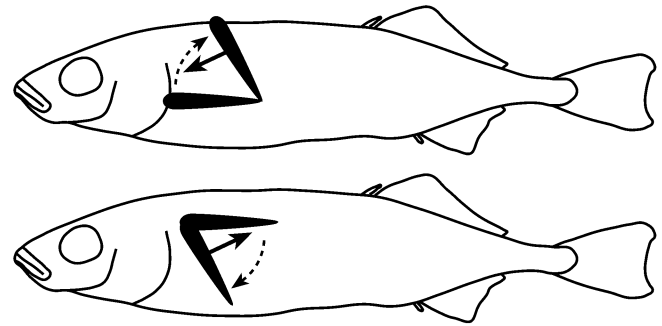


Fig. 3. Hypothetical forces on a rigidly rotating fin at the stroke transition from the recovery to power stroke in the three-spine stickleback. The black streamlined object is a cross section (chord) of the pectoral fin rigidly rotating from its feathered (horizontal) to broadside (vertical) orientation. The dashed arrows show the direction of the rotation. In the top panel, the fin is rotating about its trailing edge, which will produce a net force (solid arrow) that is oriented forward and down. In the bottom panel, the fin is rotating about the leading edge, which will produce a net force (solid arrow) that is oriented backward and up. Importantly, the stickleback employs neither of these rigid rotations, but “pulls” its flexible fin up into a broadside orientation as one might pull a rug up from a floor (see Fig. 4).

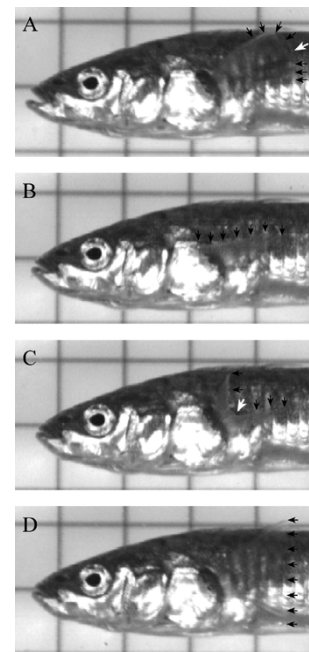


Fig. 4. Rowing stroke of the three-spine stickleback during steady swimming. (A) Fin rays, beginning with the leading edge, are sequentially “peeling” off the body during the first part of abduction. (B) Feathered orientation during the last part of abduction. (C) Beginning of adduction. As the leading edge actively adducts, inactive posterior rays sequentially activate and adduct with the leading edge. The rays dorsal to the white arrow are being actively pulled up and back. (D) End of adduction as the fin closes against the body.

to the geometry of Fig. 3). However, in this latter example, the presence of the body would limit the rate of counterclockwise rotation (because the fin cannot rotate into the body) and, with limited rotational speed, the net force would be upward, medial, and backward. If a fish is near neutral buoyancy, these vertical force components during rigid fin rotation would represent wasted energy.

The spanwise twisting mechanism of pitch control in the stickleback enables this fish to avoid the large vertical forces during the rotational phases (Fig. 4). Immediately prior to the

recovery stroke in the stickleback, the fin rotates counterclockwise along the body. The first part of the recovery stroke is characterized by the fin rays peeling off the body, starting with the leading edge ray and proceeding, ray by ray, to the trailing edge ray. As the leading edge rays peel off the body, the trailing rays continue to rotate counterclockwise along the body. The point marked by the white arrow in Fig. 4 illustrates the break point along the distal edge separating the hydrodynamically active leading-edge region from the inactive trailing region. The trailing edge ray peels off the body about the time it reaches the same dorsoventral position as the leading edge ray. The second part of the recovery stroke is characterized by the fin translating anteriorly with the plane of the fan pitched slightly ventrally (Fig. 4).

The power stroke of the stickleback begins with a rapid dorso-caudal translation of the leading edge ray. The dorsal translation of the leading edge causes a clockwise rotation of the anterior fin surface into a broadside orientation (Fig. 4). A wave of fin-ray rotation passes posteriorly as the leading edge rays translate posteriorly. During the posterior translation of the leading edge surface, the trailing rays stopped translating anteriorly, but may move slightly ventrally. The white arrow in Fig. 4 illustrates the break point on the distal edge marking the leading edge region, which is rapidly translating posteriorly, from the trailing edge region, which has largely stopped translating. During this time, the fin is sharply curved at this break point. It is important to note that the fin does not rigidly rotate into a broadside orientation, but instead resembles the peeling of a carpet off a floor by pulling one end back and up. Following rotation, all fin rays simultaneously translated back toward the body (Fig. 4). A similar pattern of fin ray peeling during the transitions between recovery and power strokes was described for the boxfish, *Ostracion meleagris* [22].

In addition to the root pitching and spanwise twisting mechanisms of pitch control during the recovery and power strokes, many animals present a third mechanism for feathering: passive appendage feathering resulting from fluid dynamic loading on the paddle or paddle elements. In small water beetles and zooplankton, the paddle is not a solid surface, but instead a central shaft supporting numerous swimming hairs [50], [53]. The joint between the hair and shaft allows fluid dynamic stresses to collapse the hairs against the shaft during the recovery stroke but extend the hairs away from the shaft during the power stroke. No rotation is necessary and the transition between power and recovery strokes is very rapid. This mechanism is scale dependent; at low Reynolds numbers, the hairy shaft effectively acts like a solid paddle because of the relatively large boundary layer surrounding each hair [54]. In larger animals with webbed feet, such as ducks and frogs, passive feathering results from fluid-dynamic powered flexion at the ankle joint.

*b) Pectoral Fin Deformations During Maneuvering Behaviors:* Despite the many recent papers on fin control of steady swimming, our understanding of fin control of maneuvering has not progressed much beyond [24]. This lack of progress may reflect the much more diverse array of motions occurring among maneuvering pectoral fins. What is especially lacking are data on the kinematic differences occurring with different levels of performance.

All fish apparently oscillate the pectoral fins during hovering in still water. Breder [24] rejected equilibrium-maintenance and fresh-water-maintenance explanations of pectoral fin movement in favor of the suggestion that pectoral fin motions balance the thrust generated by ventilating gills. Blake [55] investigated the effects of distance above the floor on the frequency and amplitude of undulatory motions of the hovering pectoral fins of the mandarin fish *Synchropus picturatus*, but there is not enough of a qualitative or quantitative description of fin deformations to understand how the fore-aft forces cancel and how the fin generates a net upward force that balances the weight of the body. The rainbow trout, *Oncorhynchus mykiss*, oscillates its ventrally positioned pectoral fins at high attack angles in a largely sagittal plane [39]. On the abduction (protraction) stroke, drag generated on the fin due to a large flow separation and the creation of an attached vortex on the downstream surface contributes to drag at the center of mass. Because the fins alternate out of phase, the opposite-side adducting (retracting) fin should generate a similar separation, vortex formation, and resulting drag that, acting as thrust at the center of mass, balances the fore-aft forces. An attached vortex on the downstream surface of the adducting fin is not visible in the photo.

During hovering in the three-spine stickleback, *Gasterosteus aculeatus*, the pectoral fin rays oscillate anteroposteriorly with a large phase lag between leading and trailing edge (personal observation). A wave is passed from the leading (dorsal) to trailing (ventral) edge, creating a large positive angle of attack (around  $45^\circ$ ) relative to the horizontal in both abduction (forward) and adduction (backward) strokes. The large angle of attack and the ventrally propagating wave generate an upward force that balances the negative buoyancy of the fish while the symmetry in the angle of attack between abduction and adduction strokes cancels fore-aft forces.

Breder [24] suggested that pectoral fins generate turning moments and centripetal forces by one of two mechanisms. First, the inside fin (that on the inside of the turn) is held against the body while the outside fin (that on the outside of the turn) oscillates as in steady swimming; the thrust generated by the fin contributes to the rotational torque on the center of mass. Second, the outside fin is held against the body while the inside fin is extended laterally; the drag generated by the fin contributes to the rotational torque on the center of mass.

Blake [23] illustrated the adduction (or powerstroke) of the outside pectoral fin in a yaw turn of the boxfish, *Tetrasomus gibbosus*. The illustration Fig. 2 shows the fin adducting toward the body with the geometric angle of attack remaining relatively constant around a value of  $25^\circ$ . Simultaneously, a moderate-amplitude wave is passed from the leading (dorsal) to trailing (ventral) edge. According to [23], the inside fin is either held against the body or oscillates with the reverse motions of the outside fin.

Some observations on the deformations of the pectoral fins during yaw turning in the boxfish, *Ostracion meleagris*, can add to this description. In the  $195^\circ$  turn illustrated in [56, Fig. 3], the outside fin makes five full fin-beat cycles while the inside fin makes two full cycles. The outside fin strokes are similar to the steady swimming stroke described for the stickleback, except that each stroke is of large amplitude (the leading edge abducts

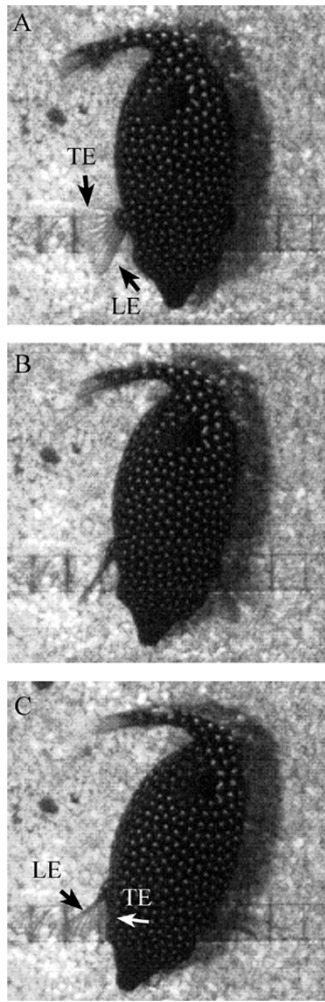


Fig. 5. Power stroke of the inside fin during a turn in the boxfish, *Ostracion meleagris*. (A) The fin is in a feathered orientation with the leading edge (LE) ray maximally abducted of all rays (note that in some fin strokes during turns, the fin can be feathered opposite to that shown here; that is, with the leading edge minimally abducted and the trailing edge ray maximally abducted). (B) The fin has rotated (supinated) about the leading edge, causing the trailing edge to abduct and the fin to enter a broadside orientation. In (C), the trailing edge (TE) ray has continued to abduct to a position greater than  $180^\circ$  so that it is now more abducted than the leading edge ray.

to about  $165^\circ$  from a posteriorly oriented vector). The drag created by the power stroke of the fin contributes to the rotational torque about the center of mass. For the first  $90^\circ$  of the turn, the inside fins remains extended in a roughly feathered orientation with the leading edge abducted about  $116^\circ$  and the trailing edge about  $25^\circ$  (Fig. 5). From this abducted feathered position, the inside fin stiffly supinates about an axis near the leading edge, which should produce a large drag (and upward) component on the fin that adds to the rotational torque. During this rotation phase, the fin rays abduct; at the end of the rotation and abduction, the leading edge is  $158^\circ$  abducted while the trailing edge is  $190^\circ$  abducted (the sharply angled lateral wall of the body anterior to the pectoral fin allows this hyperabducted motion, although it is not clear if muscle shortening or inertial forces cause the hyperabduction; Fig. 5). Following the supination and abduction, the inside fin adducts and pronates about an axis close to the leading edge. The pronation is not a stiff-plate rotation (as in the supination), but is executed as a wave (similar to the

rotation phase described for the stickleback pectoral fin), which presumably generates less drag on the fin (which would subtract from the rotational torque). At the end of the pronation phase, the inside fin has returned to a feathered orientation with the leading edge at  $150^\circ$  and the trailing edge at  $33^\circ$ . The inside fin makes a second beat that starts with a stiff supination about the  $1/4$  chord axis. At the end of this supination, the leading edge has adducted to  $95^\circ$  while the trailing edge is at  $130^\circ$ . This second supination is followed by a stiff pronation into a feathered orientation. The stiff pronation should generate a downward and forward force that both slows rotation and increases acceleration away from the turn. Finally, it should be noted that, in some turns, the inside fin executes a feathered adduction stroke led by the leading edge ray (requiring a large spanwise twist).

The bluegill sunfish, *Lepomis macrochirus*, uses both inside and outside pectoral fins to generate small turning moments at low swimming speeds [57]. Peak rotational velocity occurs when the outside fin rapidly adducts from an initially strongly abducted position, while the ipsilateral fin slowly adducts from an initially weakly abducted position. Both the inertial force at the beginning and the circulatory force at the middle of the outside fin adduction stroke should contribute to the rotational torque. During its initial abducted position, it may generate drag that contributes to the torque. The large posteriorly directed jet that develops by the end of the stroke, however, suggests that the fin, at least during adduction, creates a torque of opposite sign, which may serve to brake the rotation.

### III. PERFORMANCE

Maneuvering behaviors are composed of one or more measurable whole-animal performances, such as braking acceleration, turning radius, turning rate, etc. Whole-animal performance, in turn, is a function of multiple interacting physiological systems influencing the ability of the fish to deform multiple control surfaces, of fluid dynamic and inertial properties of the body and control surfaces, and of fluid dynamic interactions among control surfaces and between control surfaces and the body. Experimental and computational investigation of control-surface performance within isolated and interacting model fins is reviewed in more detail in [2] and [3] while aspects of whole-animal performance from a quantitative wake visualization perspective is reviewed in [1]. In this section, I will concentrate on measures of whole-animal performance components and how these are related to control-surface performance. The review is limited to yaw-turning performance, because there are too few data from other types of maneuvering for comparison. The only comprehensive study of a wide variety of maneuvering performances is [8].

Yaw turns are actuated by creating a net turning moment, or torque, about a dorsoventral axis that runs through the center of mass. Turns are powered by some combination of passive and active control surfaces. A passive control surface (a fin or region of the body) held at an angle to the local flow creates an asymmetric pressure distribution over the surface and a turning moment about the axis of rotation. The energy for passive (or trimmed) turn arises from the kinetic energy of the moving fish (or moving water if the control surface is held in a current). An

actively moved control surface generates both circulatory (drag and lift) and inertial forces that, in turn, contribute to the net turning moment about the axis of rotation. The energy for an active (or powered) turn arises from the work of the muscles actuating the control surface.

#### A. Yaw-Turning Performance Measures

For fishes, as with AUVs, there is no single best measure of turning performance. High linear and rotational velocities and accelerations should augment evasive maneuvers from predators. The ability to rapidly and precisely reposition one's orientation over a broad range of angular displacements should facilitate inspection behavior (scanning a territory, searching for prey) and correct for small perturbations to the heading. Low turning radius turns should increase the ability of fishes to exploit resources in structurally complex environments such as submerged vegetation or coral reefs. Turning with high efficiency saves energy that could be allocated to other functions or behaviors. None of these variables have been measured in any single study. Some, such as the ability to precisely reposition one's orientation, are poorly defined, do not have an easily measured performance, and have not been measured. Others, such as rotational accelerations, are easily defined and measured, but have not been reported in any study. Still others, such as turning with high efficiency, have been measured in behaviors (fast-start escape responses) in which efficiency is unlikely to be the performance variable that the deforming body is optimizing.

Two types of turning-performance measures have been explored: translational variables, which are some function of the linear displacement of the center of mass, and rotational variables, which are some function of the angular displacement of the anterior body (the line segment in the median sagittal plane connecting the anterior tip of the snout and the stretched-straight center of mass). Rotational variables have been estimated from center of mass displacement but in boxfish, at least, the duration of body rotation can be much longer than the duration of body translation around a turning arc [56].

Translational variables that have been reported include maximum linear velocity and acceleration, minimum coefficient of normal acceleration, and minimum turning radius. The coefficient of normal acceleration [58] is the gravity-standardized acceleration normal to the turning path. While the turning radius is always reported as a single number, the radius of curvature along a turning path is generally not constant (Fig. 6). Walker [56] used numerical differentiation to estimate instantaneous radius of curvature along the turning path of boxfish and reported the minimum radius along the path as the measure of maximum performance. At least for boxfish, this is somewhat unsatisfying, as the minimum radius does not capture the shape of the turning curve. More recently, Walker (unpublished data) computed the major and minor axes of the turning path and used these as additional performance variables (Fig. 6).

Peak rotational acceleration  $\alpha_{\max}$  during a turn would be a useful variable for comparison, since it is most directly related to control surface performance (net maximum torque generated by the control surfaces), but  $\alpha_{\max}$  for any fish has yet to be reported. Peak rotational velocity  $\omega_{\max}$  has been reported and is closely related to control surface performance if the duration of

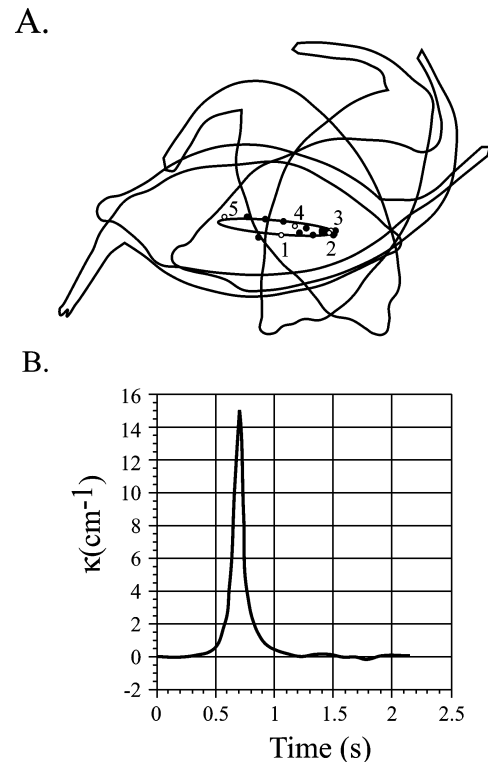


Fig. 6. Turning of the boxfish, *Ostracion meleagris*. (A) Outlines of the body and the corresponding path of the center of mass illustrate that body rotation occurs both prior to and following the change in direction of the center of mass. The closed and open circles mark the path of the center of mass. The open circles are numbered to indicate the direction of the path and the associated body outline (which are not numbered, but can be easily followed). Note that the body begins to rotate well before the center of mass switches direction and, similarly, continues to rotate after the center of mass has switched direction. There is no single radius of turning curvature (see B). Instead, the magnitude of the major and minor axes of the scatter of points along the turning path (represented by the ellipse) are parameters describing the turning performance. (B) The change in the curvature  $k$ , which is the reciprocal of the radius of curvature, along the turning path illustrated in (A). The curvature is low for most of the turn, but has a sharp peak where the center of mass sharply reversed direction.

the turn is greater than that necessary to achieve  $\omega_{\max}$ . More typically, the average rotational velocity over a turn  $\omega_{\text{avg}}$  is reported.  $\omega_{\text{avg}}$  is a function of the duration of the turn in addition to the torque generated by the control surfaces and the inertial and drag resistance of the body. Variation in duration will reflect both morphophysiological differences, including differences in muscle contractile durations and inertial resistance to body deformations [59], [60] and the total angular displacement of the turn  $\Delta\theta$ . Indeed, Domenici and Blake [61] have shown a negative correlation between  $\Delta\theta$  and  $\omega_{\text{avg}}$ .

Three yaw-turn designs that are relevant to AUV and fish maneuvering are compared. Pectoral-fin (PF) turns are actuated by one or both PFs. The outside fin employs its optimal thrust-generating motion (in general, this should be a rowing motion) while the inside fin employs is optimum drag-generating motion (in general, this could be braking with an extended fin or "reverse" rowing). The fins generate a combined moment that rotates the heading of the fish toward the inside. Caudal-fin (CF) powered turns are actuated by the CF swinging about a base located somewhere along the caudal peduncle. Inertial and circulatory forces on the fin will generate large yaw torques that

will rotate the fish (note that the sign of the torque occurring at the end of the stroke will be opposite to the that occurring halfway through the stroke and at the beginning of the stroke). Caudal-body (CB) powered turns are similar to CF turns, but a flexible body swings the CB (which may include the median fins if these are posteriorly positioned) and CF about the center of mass (in general, this motion is not stiff, but is generated by a wave of bending that passes caudally).

### B. Yaw-Turning Performance Variation

1) *Turning Radius:* The most common measure of turning maneuverability is the turning radius  $R$ , which decreases with increased performance, or its reciprocal, turning curvature  $\kappa$ .  $R$  is a function of the kinetic energy of the fish and the centripetal force

$$R = \frac{mV^2}{F_c} \quad (1)$$

where  $m$  is the virtual mass (the sum of the fish and added mass),  $V$  is the tangential velocity of the center of mass, and  $F_c$  is the centripetal force, which is the sum of the components of the circulatory and inertial forces on each control surface that are normal to the heading of the fish. If we substitute into (1) the circulatory centripetal force

$$F_{c,r} = \frac{1}{2}\rho S U^2 C_N \quad (2)$$

where  $\rho$  is the density of the water,  $S$  is the area of the control surface,  $U$  is the resultant velocity of the control surface at the center of the force distribution, and  $C_N$  is the coefficient of the component of net force normal to the heading of the fish, then

$$R \propto (m/S)(V^2/U^2). \quad (3)$$

Two useful predictions can be drawn from (3). First, if the body or gliding wings or fins are generating  $F_c$ , then  $U \approx V$  and  $R$  will be independent of speed, as shown by [62]. However, if oscillating fins are contributing to  $F_c$ , then  $R$  will decrease to zero as  $V^2/U^2$  decreases to zero (or, effectively, as  $V$  decreases to zero). Second,  $R$  will scale with body length  $L$  and the relative performance  $R/L$  will be proportional to  $V^2/U^2$ . It has been argued that  $R/L$  should increase with the flexural stiffness of the body [13], [63], but the above analysis suggests that this constraint should only be relevant to turns powered by the kinetic energy of the moving body and that animals or vehicles that power turns with root-flapping fins (regardless of if the body/hull is rigid or not) should be able turn with effectively zero turning radius [56].

Because of the broad range of experimental differences among the studies, including the focal behavior (fast starts, routine turns, feeding turns) and the method of estimating the turning radius, it is difficult to test if these predictions can explain natural variation in minimum  $R$  measured among different fishes (Fig. 7). Given what data are available, three tentative conclusions are made. First, while a slope of unity is expected, the measured least squares slope though all data is 1.8, which differs significantly from 1. Because of the aforementioned variation in methodology, this value should be interpreted cautiously. Second, PF turns are expected to be sharper (lower

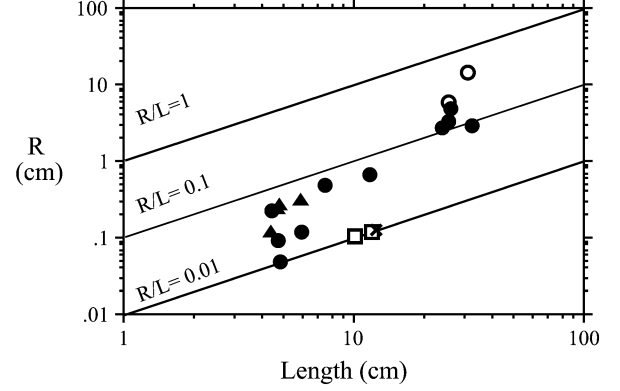


Fig. 7. Minimum turning radius measured for different fishes from CB turns (solid and open circles), pectoral fin turns (solid triangles), pectoral and median fin turns of the boxfish, *Ostracion cubicus* (open squares), and the caudal fin turn of *O. cubicus* (X). Open circles are CB turns of relatively stiff-bodied fish. The four pairs (solid circles and triangles) of data at the small end of the length scale are coral reef fishes that are pectoral fin specialists. CB turns include both routine turns and fast starts. Data is from [7], [13], [56], and unpublished data on *O. cubicus*.

$R/L$ ) than CB turns, however, at least among coral reef fishes the opposite occurs [7]. Unfortunately, it is not clear to what extent the CB turns of the coral reef fishes are using the PFs to cancel translational components (this was not described in the original paper). When this comparison is extended to all of the fishes in Fig. 7, the fishes that can use large-amplitude PF oscillation to contribute to the net turning moment have sharper turns than the fishes that do not typically use large-amplitude PF oscillation to contribute to the net turning moment. This conclusion is confounded by size, however, as all of the PF specialists were small individuals while the non-PF specialists were large individuals. Finally, for coral reef fishes that use the PFs to generate turning moments, turning radius is not a function of body stiffness (as expected; see above) [56].

2) *Linear Acceleration:* Acceleration is proportional to thrust generated by a combination of circulatory and inertial (added mass) forces. At high accelerations, the inertial component should dominate the thrust balance. This inertial component can be modeled by

$$T_i = \frac{1}{4}\pi\rho \int c^2 \dot{U}_N \beta dS \quad (4)$$

where  $c$  is the depth or chord of the control surface,  $\dot{U}_N$  is the normal acceleration of the control surface,  $\beta$  is an added mass coefficient, and  $dS$  is segment width. Increased depth (but not breadth) in regions of the control surface that have the highest normal accelerations are expected to increase acceleration [64]. Thus, we would expect distally expanding fins in fishes that use fins for accelerating water [65] and caudally positioned and deep median fins in fishes that use the CB to generate large accelerations [66]. Normal accelerations can be increased by decreasing nonmuscle mass, increasing the expression of type IIx fibers in the muscles actuating the control surface, or by increasing the mechanical advantage of the musculoskeletal system.

Maximum CB-powered accelerations have been measured for many fishes (Fig. 8), but there are no PF- or CF-powered accelerations for comparison with each other or with CB

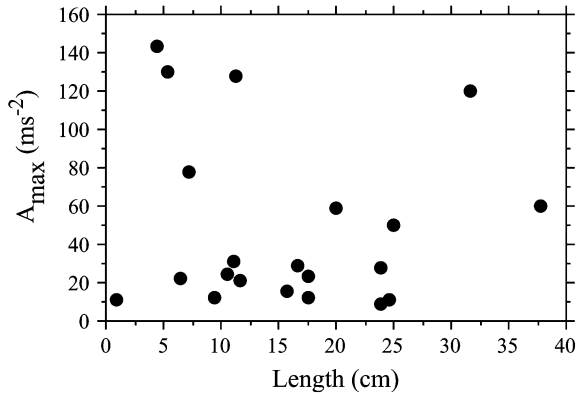


Fig. 8. Species mean maximum acceleration during fast starts for different fishes as a function of body length. Data from [59], [61], [70], [71], and [86]–[92].

turns. Kinematic and morphological factors of acceleration performance have been frequently addressed, but unambiguous results are uncommon. In general, C starts produce higher accelerations and are associated with larger turning angles than S starts [13]. Within C starts, it has been suggested that greater axial curvatures along the body at the end of stage I should produce larger accelerations and there is some evidence to support this [67]–[69]. In contrast, [70] found a negative association between acceleration performance and maximum curvature. Finally, in a comparison of C starts among six fishes, [71] found that maximum accelerations were a function of the wave speed of body bending, but not of body curvature. Morphological features that have been proposed as augmenting acceleration performance include increased body depth, decreased body depth, increased median and CF area, caudally positioned median fins, increased flexural stiffness, and reduced flexural stiffness. There are no good comparative or experimental data to support any of these hypotheses, with the exception of a fin-ablation experiment supporting the hypotheses that increased fin area in the caudal region of the body augments acceleration performance [66].

Because isometric muscle tension is proportional to  $L^2$  and the inertial resistance to acceleration is proportional to  $L^3$ , it has been assumed that maximum acceleration scales as  $L^2/L^3 = L^{-1}$ . However, the thrust available for acceleration is less a function of isometric muscle tension than with the output force of the geared musculoskeletal system [72]

$$F_{out} = F_{dyn} \frac{d_{in}}{d_{out}} \quad (5)$$

where  $F_{dyn}$  is the maximum dynamic muscle tension and  $d_{in}$  and  $d_{out}$  are the input and output lever arms, respectively. In contrast to the expectation from isometric muscle tension scaling, Marden and Allen [73] showed that  $F_{out}$  scales to  $L^3$  across a broad range of animal and human-engineered motor systems and over a tenfold range in scale. If the available force for acceleration is proportional to  $L^3$  and mass scales isometrically, then maximum acceleration should scale with an exponent of zero. Indeed, both among species (Fig. 8) and within species [74], [75], acceleration is independent of size (larval and juvenile fishes are an exception) [59], [76]. This

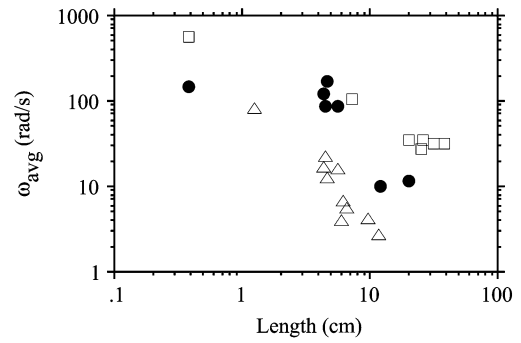


Fig. 9. Maximum average rotational velocities for different fishes during fast starts (open squares), routine CB turns (solid circles), and routine PF turns (open triangles). Data from [7], [11], [12], [56], [61], [74], [89], and [91] and unpublished data from *Ostracion cubicus*.

change in acceleration within early post-hatching ontogeny probably results from changing kinetic properties of the myotomal muscle. Allometric scaling of  $F_{dyn}$ ,  $d_{in}$ , and  $d_{out}$  has not been investigated in fishes. Among dragonflies, maximum dynamic muscle tension scaled with a length exponent of 2.52, which was significantly greater than the expected isometric scaling of 2.0 [72].

3) *Rotational Velocity*: High rotational-velocity turns are achieved by generating large forces with long moment arms. Circulatory (drag and lift) and inertial (acceleration reaction) forces, in turn, are functions of both the area of the control surface and the velocity (circulatory) or change in velocity (inertial) of the incident flow over the control surface. Three lines of evidence suggest that CB turns should be fastest. First, the center of mass of fish lies somewhere in the anterior half of the body, a position that will generally give the CB a moment arm nearly as long as the CF by itself and much longer than that of either PF. Second, peak velocities and normal accelerations of the center of force of the CB are higher than for either the PF or the CF, because the longer span of the CB and because the muscles powering CB deformations are larger and have higher proportions of fast twitch fibers than muscles powering the pectoral or CF rays. Finally, the area of the CB is larger than the areas of either the CF or PFs.

Both mean rotational velocities  $\omega_{avg}$  and peak rotational velocities  $\omega_{max}$  have been reported. A comparison of measured rotational velocities among PF-, CF-, and CB-powered turns (Fig. 9) supports the prediction that CB turns are fastest. Some of the difference between turning types is due to motivation; the PF data are from routine turns while the CB data are from both routine turns and highly stereotyped fast-start escape responses, or C starts, that are used to rapidly move the fish out of the path of a striking predator. Limiting the comparison to routine turns shows that routine CB turns are higher than PF turns (Fig. 9). For CB turns, axial bending not only increases the amplitude (and torque) of the CF, but also allows the tail and median fins to contribute to the torque. Because of their stiff bony carapace, which precludes axial bending anterior to the caudal peduncle, boxfishes provide the unusual opportunity to measure rotational velocity in CF turns in which prepeduncle axial bending cannot augment performance. In the boxfish *Ostracion cubicus*, the CF is only actively oscillated in startle ma-

neuers. Boxfish CF startle turns are faster than PF turns, but are slower than the CB C starts of more flexible fish (Fig. 9). Again, the faster CF turns relative to PF turns in *O. cubicus* should not be surprising. While fin areas and moment arms have not been measured in *O. cubicus*, [22] showed that the area of the CF is 42% greater than the summed area of both PFs in *O. meleagris*.

While axial bending should decrease both viscous and inertial resistance to rotation, estimates of rotational drag and moments of inertia for different amounts of axial deformation have not been investigated. PFs that are longer, have more of the area distributed toward the tip (i.e., higher radial moments of area about the fin base) and move with a more rowing-like motion will generate larger turning moments than fins with the opposite phenotypes [27], [65]. This suggests that fishes with fan-shaped rowing fins can generate higher PF-powered rotational velocities than can fishes with wing-shaped flapping fins. This hypothesis has not been formally tested, but a comparison of turns between boxfishes with fan-shaped fins and species of wrasse, surgeonfish, and angelfish with wing-shaped fins do not support the hypothesis. As with all comparative tests of causal hypotheses, however, the comparison is confounded by unmeasured variables and uncontrolled variation. For example, a boxfish has a larger second moment of mass (moment of inertia) than a wrasse of equal length when at rest; this difference increases during a turn because of the wrasse's ability to bend.

4) *Miscellaneous Yaw-Turning Performance*: One aspect of maneuverability is the ability to easily move within confined spaces. Based on qualitative comparisons of fishes among habitats, functional ichthyologists have generally concluded that a combination of a deep body and laterally positioned PFs facilitates maneuverability and the exploitation of resources in structurally rich habitats such as aquatic vegetation and coral reefs [77], [78]. Variation in the ability to maneuver in confined spaces was compared among goldfish (*Carassius auratus*), silver dollar (*Metynnis hypsaurchen*), and angelfish (*Pterophyllum scalare*) by coercing these fishes to negotiate slits and tubes of various geometries [79]–[81]. (It should be noted that the ability to move in an enclosed space is not the same as the ability to exploit resources in structurally complex habitats and the optimum body shapes in these habitats may radically differ. Compare the eel-shaped design of the crevice denizens with the pancake-shaped design of the fishes maneuvering among coral, but not within it.) Relative to goldfish, silver dollars and angelfish, with their deep and narrow bodies, were able to move through 63% and 45% narrower tubes per cube-root unit body mass, respectively. (Note that my interpretation of the data, which is based on standardizing by body mass, is consistent with that of [79] but differs from that of [80], which is based on standardizing by total length. I am explicitly asking the question, “given a fish with a certain unit mass, what is the best distribution of the mass itself and of fins around the mass to facilitate maneuvering through slits and tubes?”) In contrast, goldfish can turn in smaller bent tubes and the goldfish performance, relative to that of silver dollars and angelfish, increases with the magnitude of the bend [81]. While these confinement experiments ultimately failed to discover the general principles of optimal body and fin design for open-water maneuverability, they did show that expected optimal designs for open water

maneuvering are relatively poor designs for maneuvering in confined spaces (see also [56]).

#### IV. CONCLUSION AND FUTURE WORK

Evolutionary fish biologists and AUV designers interested in biology-inspired technologies share many of the same goals, such as what are the optimal body (hull) and fin (control surface) designs for different behaviors (steady forward propulsion with high efficiency; station holding or precision maneuvering in unidirectional, bidirectional, or turbulent flow; reversing) and what are the design tradeoffs in optimizing any one behavior? The repeated associations between diverse morphologies and habitats among fishes enabled Paul Webb to develop the first general theory to address these sorts of questions in fishes [77], [78]. Some of these repeated associations relevant to AUV performance include association between: 1) structurally complex habitats and fishes with short, narrow, and deep (pancake-shaped) bodies; 2) fast continuous swimming and generally moderately elongated, streamlined bodies; 3) ambush (high acceleration) piscivory and elongate, round bodies with posteriorly positioned median fins; and 4) tropical marine reefs (with generally complex structure and high energy flows) and augmented variance in pectoral and median fin morphology and function. Biologists have tended to interpret Webb's model as truth rather than using it as a guide for devising experiments to tests its many components. Consequently, despite over two decades of research on the functional biology of fish swimming following the introduction of Webb's model, we still have few direct tests of Webb's or similar models of fish design and swimming performance.

The combination of qualitative morphological and behavioral comparisons among the species, simple models, and empirical performance measurements reviewed here allows a tentative summary of causal relationships between fin shape, fin motion, and performance (Table I). This table especially highlights the tradeoffs between maneuverability and ability to cruise with high efficiency within each fin system.

The details of Table I and the tests of Webb's model are woefully incomplete. To rectify these deficiencies, biological or biology-inspired engineering research should focus on three areas. First, we need sharper definitions of the important measures of maneuverability. Broad differences in turning radius appear associated with broad behavioral differences; pelagic or migratory fishes with less-active PFs and relatively stiff bodies have higher turning radii than coral reef fishes with active PFs and/or flexible bodies. But are small (if at all) differences in turning radius part of the explanation for body-shape variation among coral reef fishes? More importantly, at least in boxfishes (see above), turning radius is a very incomplete measure of turning sharpness. Also, other than fast starts (for which it is probably less relevant), there are no studies measuring the energy required to turn or to stabilize perturbations to the heading. Keels on the body of the boxfish, *Lactophrys triqueter*, act as passive control surfaces that self-correct perturbations to the heading during steady swimming [82]. Perhaps the focus on highly maneuverable fishes should focus more on the energetic consequences of variation in control surface shape and movement.

TABLE I

SUMMARY OF FIN SHAPE, MOTION, AND FUNCTION IN TELEOST FISHES. PADDLE-SHAPED FINS ARE NARROWEST AT THE ROOT AND EXPAND DISTALLY (TOWARD THE TIP). THE PECTORAL FIN OF THE THREESPINE STICKLEBACK, THE DORSAL FIN OF THE BOXFISH, THE SOFT POSTERIOR PORTION OF THE DORSAL FIN OF THE BLUEGILL SUNFISH, AND THE CAUDAL FIN OF THE KING SALMON ARE PADDLE SHAPED. WING-SHAPED FINS ARE WIDEST NEAR THE BASE AND TAPER DISTALLY. THE PECTORAL FIN OF THE BIRD WRASSE, THE DORSAL FIN OF THE OCEAN TRIGGERFISH, AND THE CAUDAL FIN OF THE TUNA ARE WING-SHAPED. RIBBON-SHAPED FINS ARE ELONGATED WITH MUCH LONGER CHORDS THAN SPANS. THE ANAL FIN OF A KNIFEFISH IS RIBBON-SHAPED. IN GENERAL, PADDLE-SHAPED FINS PECTORAL FINS HAVE ROWING (FRONTAL PLANE) OR PADDLING (SAGITTAL PLANE) MOTION, WITH DISTINCT RECOVERY AND POWER STROKES, WHILE PADDLE-SHAPED MEDIAN AND CAUDAL FINS HAVE FAIRLY TYPICAL FLAPPING (HEAVING AND PITCHING) MOTIONS. SOME AMOUNT OF UNDULATION IS TYPICAL OF ALL PADDLE-SHAPED FINS. WING-SHAPED FINS TEND TO FLAP AND OFTEN SHOW LITTLE TO NO UNDULATION. RIBBON-SHAPED FINS ARE HIGHLY UNDULATORY. WHILE ALL FINS CAN BE USED TO ACCELERATE, THE PADDLE-SHAPED CAUDAL FINS TEND TO BE ASSOCIATED WITH FISHES THAT ARE ACCELERATION SPECIALISTS. PADDLE-SHAPED PECTORAL FINS AND BOTH PADDLE- AND RIBBON-SHAPED MEDIAN FINS ARE FOUND ON FISHES THAT EXCEL AT BRAKING, HOVERING, AND REVERSING. PADDLE-SHAPED PECTORAL FINS ARE ALSO COMMON IN FISHES THAT EXCEL AT SPINNING (YAW TURNS WITH A LOW TURNING RADIUS). WING-SHAPED PECTORAL, MEDIAN, AND CAUDAL FINS ARE MOST COMMONLY FOUND IN FISHES THAT ARE OPEN-WATER CRUISERS

Fin Shape	Pectoral		Dorsal/Anal			Caudal	
	Paddle	Wing	Ribbon	Wing	Paddle	Paddle	Wing
Motion	rowing/ paddling	flapping	undulation	flapping	flapping		
Behavior							
accelerating						*	
braking	*		*		*		
hovering	*		*		*		
reversing	*		*		*		
spinning	*				*	*	
cruising		*		*			*

Second, we need more detailed anatomical and kinematic descriptions. Important anatomical measures include fin mass, moments of fin area and mass, body mass, and moments of body and fin area and mass about each rotational axis. Kinematic descriptions that follow those for flapping insect wings (e.g., [37]) are not sufficient for fish maneuvering because of the greater complexity of fin deformations. In addition to the typically reported frequency and amplitude of the leading edge ray, stroke plane angle, and geometric angles of attack, we need better quantitative measures of fin deformations than the qualitative descriptions given for the stickleback and boxfish above. Importantly, we need these anatomical and kinematic descriptions in combination with performance measures. The former are typically collected by biomechanical physiologists that are less interested in performance and more interested in developing models of how deforming fins and bodies generate fluid dynamic forces. Performances are typically measured by ecologists who largely treat the functional morphology as a black box.

Finally, we need a highly collaborative research program integrating biology-inspired physical and computational models of oscillatory fin dynamics. The biology suggests the relevant design variation and performance consequences, but the physical and computational models are necessary to control confounding variables in tests of the causal factors of performance variation. For example, a comparison of fishes that specialize in median (dorsal and anal) fin propulsion suggests that high aspect ratio, distally tapering fins that undulate with a large wave length to maximum chord length ratio (“oscillatory fins”) should be more

effective for cruising at moderate speeds with little wasted energy, while low aspect ratio, ribbon-shaped fins that undulate with a small wave length to maximum chord length ratio (“undulatory” fins) should be more effective for complex maneuvers (reversing and pitching) [15], [17]. Similarly, a comparison among fishes that specialize in PF propulsion suggests that high aspect ratio, distally tapering, “wing-shaped” fins that flap up and down should be more effective for efficient cruising while low aspect ratio, distally diverging, “paddle-shaped” fins that row back and forth should be more effective for complex maneuvers. These inferences based on comparative data have been tested using simple numerical models [15], [16], [27], but fin design-performance relationships, which have direct relevance to AUV design, need to be investigated with more sophisticated physical and computational models. The biology suggests that highly compliant fins supported by multiple, independently actuated, stiff rods are important for achieving the desired level of control. This biology presents a stiff challenge to physical and computational modelers. The recent physical and computational models of stiff [40], [42], [83] or passive chordwise flexible [16], [84], [85] plates are not sufficient to investigate performance consequences of the design variation occurring in the pectoral and median fins of fishes. Instead, we need fin models that: 1) allow active control of both rigid body (heaving and pitching) and chordwise deformations and 2) present biologically realistic responses to elastic and fluid dynamic stresses. Computational models are more flexible than physical models for exploring large design spaces and are easier to “instrument” (measuring the distribution of velocity, vorticity or pressure), but the physical models are necessary for validating the computational models.

## REFERENCES

- [1] G. V. Lauder and E. G. Drucker, “Morphology and experimental hydrodynamics of piscine control surfaces,” *IEEE J. Oceanic Eng.*, vol. 29, pp. 556–571, July 2004.
- [2] R. Mittal, “Computational modeling in bio-hydrodynamics: Trends, challenges, and recent advances,” *IEEE J. Oceanic Eng.*, vol. 29, pp. 595–604, July 2004.
- [3] M. Triantafyllou, A. Techet, and F. Hover, “Review of experimental work in biomimetic foils,” *IEEE J. Oceanic Eng.*, vol. 29, pp. 585–594, July 2004.
- [4] P. J. Geerlink, “The role of the pectoral fins in braking of mackerel, cod, and saithe,” *Netherlands J. Zool.*, vol. 37, pp. 81–104, 1987.
- [5] J. J. Videler, *Fish Swimming*. London, U.K.: Chapman & Hall, 1993.
- [6] K. D’Aouit and P. Aerts, “A kinematic comparison of forward and backward swimming the eel *Anguilla anguilla*,” *J. Exp. Biol.*, vol. 202, pp. 1511–1521, 1999.
- [7] C. L. Gerstner, “Maneuverability of four species of coral-reef fish that differ in body and pectoral-fin morphology,” *Can. J. Zool.*, vol. 77, pp. 1102–1110, 1999.
- [8] P. W. Webb and A. G. Fairchild, “Performance and maneuverability of three species of teleostean fishes,” *Can. J. Zool.*, vol. 79, pp. 1866–1877, 2001.
- [9] G. V. Lauder, “Caudal fin locomotion in ray-finned fishes: Historical and functional analyzes,” *Amer. Zool.*, vol. 29, pp. 85–102, 1989.
- [10] D. Weihs, “A hydrodynamical analysis of fish turning manoeuvres,” *Proc. R. Soc. Lond. B*, vol. 182, pp. 59–72, 1972.
- [11] P. Domenici and R. S. Batty, “Escape behavior of solitary herring (*Clupea harengus*) and comparisons with schooling individuals,” *Marine Biol.*, vol. 128, pp. 29–38, 1997.
- [12] S. A. Budick and D. M. O’Malley, “Locomotor repertoire of the larval zebrafish: Swimming, turning, and prey capture,” *J. Exp. Biol.*, vol. 203, pp. 2565–2579, 2000.
- [13] P. Domenici and R. W. Blake, “The kinematics and performance of fish fast-start swimming,” *J. Exp. Biol.*, vol. 200, pp. 1165–1178, 1997.

- [14] M. W. Westneat, D. H. Thorsen, J. A. Walker, and M. E. Hale, "Structure, function, and neural control of pectoral fins in fishes," *IEEE J. Oceanic Eng.*, vol. 29, pp. 674–683, July 2004.
- [15] T. L. Daniel, "Forward flapping flight from flexible fins," *Can. J. Zool.*, vol. 66, pp. 630–638, 1988.
- [16] S. A. Combes and T. L. Daniel, "Shape, flapping, and flexion: Wing and fin design for forward flight," *J. Exp. Biol.*, vol. 204, pp. 2073–2085, 2001.
- [17] L. J. Rosenberger, "Pectoral fin locomotion in batoid fishes: Undulation versus oscillation," *J. Exp. Biol.*, vol. 204, pp. 379–394, 2001.
- [18] B. Wright, "Form and function in aquatic flapping propulsion: Morphology, kinematics, hydrodynamics, and performance of the triggerfishes (Tetraodontiformes: Balistidae)," Ph.D. dissertation, Univ. Chicago, Chicago, IL, 2000.
- [19] E. G. Drucker and G. V. Lauder, "Locomotor function of the dorsal fin in teleost fishes: Experimental analysis of wake forces in sunfish," *J. Exp. Biol.*, vol. 204, pp. 2943–2958, 2001.
- [20] M. S. Gordon, I. Plaut, and D. Kim, "How puffers (*Tetraodontidae*) swim," *J. Fish Biol.*, vol. 49, pp. 319–328, 1996.
- [21] V. I. Arreolla and M. W. Westneat, "Mechanics of propulsion by multiple fins: Kinematics of aquatic locomotion in the burrfish (*Chilomycterus schoepfi*)," *Proc. R. Soc. Lond., B*, vol. 263, pp. 1689–1696, 1996.
- [22] J. R. Hove, L. M. O'Bryan, M. S. Gordon, P. W. Webb, and D. Weihs, "Boxfishes (*Teleostei: Ostraciidae*) as a model system for fishes swimming with many fins: Kinematics," *J. Exp. Biol.*, vol. 204, pp. 1459–1471, 2001.
- [23] R. W. Blake, "On ostraciiform locomotion," *J. Marine Biol. Assoc. United Kingdom*, vol. 57, pp. 1047–1055, 1977.
- [24] C. M. Breder, Jr., "The locomotion of fishes," *Zoologica*, vol. 4, pp. 159–291, 1926.
- [25] R. W. Blake, "Median and paired fin propulsion," in *Fish Biomechanics*, P. W. Webb and D. Weihs, Eds. New York: Praeger, 1983, pp. 214–247.
- [26] S. Vogel, *Life in Moving Fluids*, 2nd ed. Princeton, NJ: Princeton Univ. Press, 1994.
- [27] J. A. Walker and M. W. Westneat, "Mechanical performance of aquatic rowing and flying," *Proc. R. Soc. Lond. B*, vol. 267, pp. 1875–1881, 2000.
- [28] —, "Kinematics, dynamics, and energetics of rowing and flapping propulsion in fishes," *Integr. Comparative Biol.*, vol. 42, pp. 1032–1043, 2002.
- [29] C. J. Fulton, D. R. Bellwood, and P. C. Wainwright, "The relationship between swimming ability and habitat use in wrasses (*Labridae*)," *Marine Biol.*, vol. 139, pp. 25–33, 2001.
- [30] D. R. Bellwood and P. C. Wainwright, "Locomotion in labrid fishes: Implications for habitat use and cross-shelf biogeography on the Great Barrier Reef," *Coral Reefs*, vol. 20, pp. 139–150, 2001.
- [31] P. C. Wainwright, D. R. Bellwood, and M. W. Westneat, "Ecomorphology of locomotion in labrid fishes," *Environ. Biol. Fishes*, vol. 65, pp. 47–62, 2002.
- [32] P. J. Geerlink, "The anatomy of the pectoral fin in Sarotherodon niloticus trewavas (*Cichlidae*)," *Netherlands J. Zool.*, vol. 29, pp. 9–32, 1979.
- [33] P. W. Webb, "Kinematics of pectoral fin propulsion in *Cymatogaster aggregata*," *J. Exp. Biol.*, vol. 59, pp. 697–710, 1973.
- [34] P. J. Geerlink, "Pectoral fin kinematics of *Coris formosa* (*Teleostei, Labridae*)," *Netherlands J. Zool.*, vol. 33, pp. 515–531, 1983.
- [35] A. Gibb, B. C. Jayne, and G. V. Lauder, "Kinematics of pectoral fin locomotion in the bluegill sunfish *Lepomis macrochirus*," *J. Exp. Biol.*, vol. 189, pp. 133–161, 1994.
- [36] G. V. Lauder and B. C. Jayne, "Pectoral fin locomotion in fishes: Testing drag-based models using three-dimensional kinematics," *Amer. Zool.*, vol. 36, pp. 567–581, 1996.
- [37] J. A. Walker and M. W. Westneat, "Labriform propulsion in fishes: Kinematics of flapping aquatic flight in the bird wrasse *Gomphosus varius* (*Labridae*)," *J. Exp. Biol.*, vol. 200, pp. 1549–1569, 1997.
- [38] —, "Performance limits of labriform propulsion and correlates with fin shape and motion," *J. Exp. Biol.*, vol. 205, pp. 177–187, 2002.
- [39] E. G. Drucker and G. V. Lauder, "Function of pectoral fins in rainbow trout: Behavioral repertoire and hydrodynamic forces," *J. Exp. Biol.*, vol. 206, pp. 813–826, 2003.
- [40] M. H. Dickinson, F.-O. Lehmann, and S. P. Sane, "Wing rotation and the aerodynamic basis of insect flight," *Sci.*, vol. 284, pp. 1954–1960, 1999.
- [41] N. Kato and H. Liu, "Load characteristics of a three-motor-driven mechanical pectoral fin," *J. Fluids Eng.*, 2003.
- [42] N. Kato and H. Liu, "Optimization of motion of a mechanical pectoral fin," *JSME Int. J.*, ser. C, vol. 46, pp. 1356–1362, 2003.
- [43] P. J. Geerlink, "Pectoral fin morphology: A simple relation with movement pattern?," *Netherlands J. Zool.*, vol. 39, pp. 166–193, 1989.
- [44] D. Adriaens, D. Decluyre, and W. Verrees, "Morphology of the pectoral girdle in *Pomatoschistus lozanoi* de Buen, 1923 (*Gobiidae*), in relation to pectoral fin adduction," *Belgian J. Zool.*, vol. 123, pp. 135–157, 1993.
- [45] J. A. Walker, "Functional morphology and virtual models: Physical constraints on the design of oscillating wings, fins, legs, and feet at intermediate Reynolds numbers," *Integr. Comparative Biol.*, vol. 42, pp. 232–242, 2002.
- [46] M. H. Dickinson, F. O. Lehmann, and K. G. Götz, "The active control of wing rotation by *Drosophila*," *J. Exp. Biol.*, vol. 182, pp. 173–189, 1993.
- [47] F. E. Fish, R. V. Baudinette, P. B. Frappell, and M. P. Sarre, "Energetics of swimming by the platypus *Ornithorhynchus anatinus*: Metabolic effort associated with rowing," *J. Exp. Biol.*, vol. 200, pp. 2647–2652, 1997.
- [48] C. M. Pace, R. W. Blob, and M. W. Westneat, "Comparative kinematics of the forelimb during swimming in red-eared slider (*Trachemys scripta*) and spiny softshell (*Apalone spinifera*) turtles," *J. Exp. Biol.*, vol. 204, pp. 3261–3271, 2001.
- [49] G. Hughes, "The co-ordination of insect movements. 3. Swimming in *Dytiscus*, *Hyrophilus*, and a dragonfly nymph," *J. Exp. Biol.*, vol. 35, pp. 567–583, 1958.
- [50] W. Nachtigall, "Locomotion: Mechanics and hydrodynamics of swimming in aquatic insects," in *The Physiology of Insecta*, M. Rockstein, Ed. New York: Academic, 1974, vol. III, pp. 381–432.
- [51] S. Sane and M. H. Dickinson, "The control of flight force by a flapping wing: Lift and drag production," *J. Exp. Biol.*, vol. 204, pp. 2607–2626, 2001.
- [52] J. A. Walker, "Rotational lift: Something different or more of the same?," *J. Exp. Biol.*, vol. 205, pp. 3783–3792, 2002.
- [53] T. A. Williams, "A model of rowing propulsion and the ontogeny of locomotion in *Artemia* larvae," *Biolog. Bull.*, vol. 187, pp. 164–173, 1994.
- [54] M. A. R. Koehl, "Hairy little legs: Feeding, smelling, and swimming at low Reynolds numbers," *Contemp. Math.*, vol. 141, pp. 33–47, 1993.
- [55] R. W. Blake, "The swimming of the mandarin fish *Synchropus picturatus* (*Callionymidae: Teleostei*)," *J. Marine Biolog. Assoc. United Kingdom*, vol. 59, pp. 421–428, 1979.
- [56] J. A. Walker, "Does a rigid body limit maneuverability?," *J. Exp. Biol.*, vol. 203, pp. 3391–3396, 2000.
- [57] E. G. Drucker and G. V. Lauder, "Wake dynamics and fluid forces of turning maneuvers in sunfish," *J. Exp. Biol.*, vol. 204, pp. 431–442, 2001.
- [58] P. R. Bandyopadhyay, J. M. Castano, J. Q. Rice, W. Philips, W. H. Nederman, and W. K. Macy, "Low-speed maneuvering hydrodynamics of fish and small underwater vehicles," *J. Fluids Eng.*, vol. 119, pp. 136–144, 1997.
- [59] J. M. Wakeling, K. M. Kemp, and I. A. Johnston, "The biomechanics of fast-starts during ontogeny in the common carp *Cyprinus carpio*," *J. Exp. Biol.*, vol. 202, pp. 3057–3067, 1999.
- [60] P. Domenici, "Scaling the locomotor performance of aquatic vertebrates during predator-prey interactions: From fish to killer whales," *Comp. Biochem. Physiol.*, vol. 131, pp. 169–182, 2001.
- [61] P. Domenici and R. W. Blake, "The kinematics and performance of the escape response in the angelfish (*Pterophyllum eimekei*)," *J. Exp. Biol.*, vol. 156, pp. 187–205, 1991.
- [62] P. W. Webb, "Speed, acceleration, and manoeuvrability of two teleost fishes," *J. Exp. Biol.*, vol. 102, pp. 115–122, 1983.
- [63] F. E. Fish, "Performance constraints on the maneuverability of flexible and rigid biological systems," presented at the 11th Int. Symp. Unmanned Untethered Submersible Technology, Durham, NH, 1999.
- [64] D. Weihs, "Design features and mechanics of axial locomotion in fish," *Amer. Zool.*, vol. 29, pp. 151–160, 1989.
- [65] R. W. Blake, "Influence of pectoral fin shape on thrust and drag in labriform locomotion," *J. Zool.*, vol. 194, pp. 53–66, 1981.
- [66] P. W. Webb, "Effects of median-fin amputation on fast-start performance of rainbow trout (*Salmo gairdneri*)," *J. Exp. Biol.*, vol. 68, pp. 123–135, 1977.
- [67] E. B. Taylor and J. D. McPhail, "Prolonged and burst swimming in anadromous and freshwater threespine stickleback, *Gasterosteus aculeatus*," *Can. J. Zool.*, vol. 64, pp. 416–420, 1986.
- [68] G. M. Andraso and J. N. Barron, "Evidence for a trade-off between defensive morphology and startle-response performance in the brook stickleback (*Culaea inconstans*)," *Can. J. Zool.*, vol. 73, pp. 1147–1153, 1995.
- [69] G. M. Andraso, "A comparison of startle response in two morphs of the brook stickleback (*Culaea inconstans*): Further evidence for a trade-off between defensive morphology and swimming ability," *Evolut. Ecol.*, vol. 11, pp. 83–90, 1997.

- [70] M. W. Westneat, M. E. Hale, M. J. McHenry, and J. H. Long, Jr., "Mechanics of the fast-start: Muscle function and the role of intramuscular pressure in the escape behavior of *Amia calva* and *Polypterus palmas*," *J. Exp. Biol.*, vol. 201, pp. 3041–3055, 1998.
- [71] J. M. Wakeling and I. A. Johnston, "Muscle power output limits fast-start performance in fish," *J. Exp. Biol.*, vol. 201, pp. 1505–1526, 1998.
- [72] R. J. Schilder and J. H. Marden, "A hierarchical analysis of the scaling of force production by dragonfly flight motors," *J. Exp. Biol.*, vol. 207, pp. 767–776, 2004.
- [73] J. H. Marden and L. R. Allen, "Molecules, muscles, and machines: Universal performance characteristics of motors," in *Proc. Nat. Academy of Sciences*, vol. 99, 2002, pp. 4161–4166.
- [74] P. W. Webb, "The effect of size on the fast-start performance of rainbow trout, *Salmo gairdneri*, and a consideration of piscivorous predator–prey interactions," *J. Exp. Biol.*, vol. 65, pp. 157–177, 1976.
- [75] P. Domenici and R. W. Blake, "The effect of size on the kinematics and performance of angelfish (*Pterophyllum eimekei*) escape responses," *Can. J. Zool.*, vol. 71, pp. 2319–2326, 1993.
- [76] M. E. Hale, "Locomotor mechanics in early life history: Effects of size and ontogeny on fast-start performance in salmonid fishes," *J. Exp. Biol.*, vol. 202, pp. 1465–1479, 1999.
- [77] P. W. Webb, "Locomotor patterns in the evolution of actinopterygian fishes," *Amer. Zool.*, vol. 22, pp. 329–342, 1982.
- [78] —, "Body form, locomotion, and foraging in aquatic vertebrates," *Amer. Zool.*, vol. 24, pp. 107–120, 1984.
- [79] P. W. Webb, G. D. LaLiberte, and A. J. Schrank, "Do body and fin form affect the maneuverability of fish traversing vertical and horizontal slits?," *Environ. Biol. Fishes*, vol. 46, pp. 7–14, 1996.
- [80] A. J. Schrank and P. W. Webb, "Do body and fin form affect the abilities of fish to stabilize swimming during maneuvers through vertical and horizontal tubes?," *Environ. Biol. Fishes*, vol. 53, pp. 365–371, 1998.
- [81] A. J. Schrank, P. W. Webb, and S. Mayberry, "How do body and paired-fin positions affect the ability of three teleost fishes to maneuver around bends?," *Can. J. Zool.*, vol. 77, pp. 203–210, 1999.
- [82] I. K. Bartol, M. Gharib, D. Weihs, P. W. Webb, J. R. Hove, and M. Gordon, "Hydrodynamic stability of swimming in ostraciid fishes: Role of the carapace in the smooth trunkfish *Lactophys triquetter* (*Teleostei: Ostraciidae*)," *J. Exp. Biol.*, vol. 206, pp. 725–744, 2003.
- [83] Z. J. Wang, "Two dimensional mechanism for insect hovering," *Phys. Rev. Lett.*, vol. 85, pp. 2216–2219, 2000.
- [84] J. Katz and D. Weihs, "Hydrodynamic propulsion by large amplitude oscillation of an airfoil with chordwise flexibility," *J. Fluid Mech.*, vol. 88, pp. 485–497, 1978.
- [85] M. Kemp, B. Hobson, and C. Pell, "Energetics of the oscillating fin thruster," presented at the Proc. 13th Int. Symp. Unmanned Untethered Submersible Technology, Durham, NH, 2003.
- [86] G. K. Temple and I. A. Johnston, "Testing hypotheses concerning the phenotypic plasticity of escape performance in fish of the family Cottidae," *J. Exp. Biol.*, vol. 201, pp. 317–331, 1998.
- [87] T. C. Law and R. W. Blake, "Comparison of fast-start performances of closely related, morphologically distinct threespine sticklebacks (*Gasterosteus spp.*)," *J. Exp. Biol.*, vol. 199, pp. 2595–2604, 1996.
- [88] A. K. Gamperl, D. L. Schnurr, and E. D. Stevens, "Effect of sprint-training protocol on acceleration performance in rainbow trout (*Salmo gairdneri*)," *Can. J. Zool.*, vol. 69, pp. 578–582, 1991.
- [89] D. G. Harper and R. W. Blake, "Fast-start performance of rainbow trout *Salmo gairdneri* and northern pike *Esox lucius*," *J. Exp. Biol.*, vol. 150, pp. 321–342, 1990.
- [90] M. A. Kasapi, P. Domenici, R. W. Blake, and D. Harper, "The kinematics and performance of escape responses of the knifefish *Xenomystus nigri*," *Can. J. Zool.*, vol. 71, pp. 189–195, 1993.
- [91] I. L. Y. Spierts and J. L. van Leeuwen, "Kinematics and muscle dynamics of C- and S-starts of carp (*Cyprinus carpio L.*)," *J. Exp. Biol.*, vol. 202, pp. 393–406, 1999.
- [92] E. Tytell and G. V. Lauder, "The C-start escape response of *Polypterus senegalus*: Bilateral muscle activity and variation during stage 1 and 2," *J. Exp. Biol.*, vol. 205, pp. 2591–2603, 2002.



**Jeffrey A. Walker** received the B.A. degree in geological sciences from the University of Pennsylvania, Philadelphia, in 1988 and the Ph.D. degree in anatomical sciences from Stony Brook University, Stony Brook, NY, in 1995.

He was a National Science Foundation Postdoctoral Research Fellow with Dr. Mark W. Westneat at the Field Museum of Natural History, Chicago, IL. He then continued his postdoctoral research with a contract from the Office of Naval Research. Since 2000, he has been an Assistant Professor of Biological Sciences at the University of Southern Maine, Portland. He is currently pursuing a research program on the constraints of optimizing whole animal and muscle performance of swimming and flying animals.